Journal of Microscopy, Vol. 229, Pt 3 2008, pp. 469–474
Received 29 September 2006; accepted 16 June 2007

Near-field investigation of porous silicon photoluminescence modification after oxidation in water

M. JUAN, J.-S. BOUILLARD*, J. PLAIN, G. LERONDEL, P. M. ADAM, R. BACHELOT & P. ROYER
ICD CNRS FRE 2848, Univ. de Technologie de Troyes, Laboratoire de Nanotechnologie et d' Instrumentation Optique, 12 rue Marie Curie, BP 2060, 10010 Troyes Cedex, France

Key words. Oxidation, porous silicon, SNOM.

Summary

We report on local photo-induced oxidation of porous silicon in water at room temperature. Starting from a nonluminescent sample, the oxidation process induces luminescence which was found to first increase and then decrease as a function of the oxidation time. A clear blue shift is also observed. This effect is believed to be owing to size modification of silicon nanocrystallites and thus is explained in terms of quantum confinement. Optical near-field images and spectrum are used to monitor the photoluminescence modifications after oxidation. As the photoluminescence can be widely tuned in wavelength and intensity, this method offers a way to pattern the emission properties of the sample.

Introduction

The photoluminescence (PL) of porous silicon (PSi) has been widely studied during the last decade. Several models were proposed to explain this property. The most extensively used is the quantum confinement model initially proposed by Canham (1990). This model takes into account quantum size effect on the silicon band gap and the momentum conservation rules. Although a wide range of experiments can be explained with this model it appears clearly that the surface and more especially the native oxidation has to be also taken into account. This was confirmed in 1999 by the experiment conducted by Wolkin *et al.* (1999). They show that, by simple chemical dissolution in hydrofluoric solution (HF), the luminescence can be tuned from Neon infrared (NIR) to the ultraviolet (UV) as long as the sample has never been exposed to air (not oxidized). Often expected, this effect has only been observed in the past *in situ* in liquid phase in HF (Bsiesy *et al.*, 1993). Although in both cases the size reduction of the nanocrystallites and thus quantum confinement explains the blue shift of the emission, Wolkin *et al.* shows that for a nanocrystallite size typically smaller than 2 nm, the emission is no longer size dependent but is fixed by the native oxide layer. In addition to surface effects, the relation between the nanocrystallite size and PL is further complicated by the fact that in PSi, the nanocrystallite are linked together forming a network and that carrier tunnelling between the crystallites can also occur (Vial *et al.*, 1992).

As already mentioned, PL can be tuned chemically by dissolution in HF. Depending on the intrinsic carrier concentration this effect can be strongly influenced by light (photo dissolution). To minimize this effect, PSi is usually anodized in the dark. However combined with well-defined illumination patterns it has been shown that photo dissolution can be used to selectively modify PSi properties such as porosity, refractive index and PL (Lerondel *et al.*, 1997a,b). First demonstrated on the micrometre scale by holography in the visible, PS photo-induced patterns have later been obtained at the submicrometre scale using near-field optics (Diesinger *et al.*, 2002), however, with the difficulty of using glass fibre in HF. Beside photo dissolution in HF, it is also well known that PSi photoluminescence can be drastically modified when exposed to air. The oxidation process is believed to be responsible for these changes. Thus, various environmental parameters and their effects on the ageing of the material have been investigated. To mention one, the illumination during ageing induces strong modification of the PL spectrum. For example samples stored in dark show a slight modification of their emissions properties compared with those stored under light (Canham, 1990). These results suggest that PL can be widely modified by photo oxidation (Koropecki *et al.*, 2004). We recently reported on local photo oxidation of PSi in water (Juan

Correspondence to: J. Plain. Tel: +33 3 25 71 84 48; fax: +33 3 25 71 84 56; e-mail: jerome.plain@utt.fr

*Actual address: Center for Nanostructured Media, School of Mathematics and Physics, Queen's University of Belfast, University Road, Belfast BT7 1NN, U.K.

et al., 2007). Compared with photo-induced dissolution (in HF atmosphere), photo oxidation can be performed in 'inert' atmosphere (air; water) and thus, can be seen as a soft process.

In this paper, we investigate further the mechanism at the origin of the photo-induced pattern and perform near-field characterization. The use of water as oxidation medium rather than air was mainly motivated by the oxygen concentration. PSi samples are immersed in water and exposed under various illumination patterns. Both scanning near-field optical microscopy (SNOM) and atomic force microscopy (AFM) have been used to image the obtained photo-generated structures. The SNOM offers a way to locally investigate the emission properties of the PSi after oxidation. Moreover, we used a spectrometer coupled to the SNOM to analyse local spectrum of the PL. In addition, AFM provides information on the topographic modification of the sample.

Materials and methods

PSi substrate preparation

PSi samples have been prepared by electrochemical etching in HF. The back face of the silicon substrate is gold coated to be conductive. The second electrode is circular shaped, immersed in the electrolyte. The current density is maintained constant using a current generator. Depending on formation parameters, pore size, porosity and layer thickness can be adjusted. PSi substrates have been classified depending on the pore size of the porous layer: microporous or nanoporous (<2 nm), mesoporous (2–50 nm) and macroporous (>50 nm) (Cullis *et al.*, 1997). P-doped silicon substrates are used for the formation of nanoporous silicon layer. Because the main point of this study is the PL of the PSi sample and its modification after oxidation, only p-doped silicon substrates (1.5–2 ohmcm) have been used here. Experiments have been conduced on two main different types of samples. Type A samples were anodized for 20 s in a 35 : 30 : 35 HF : ethanol : H_2O solution using a 16.6 mA/cm^2 current density. Type B samples were anodized in the same condition but for 3 min. The porosity of type A and B sample is 51%. Further details about anodization can be found elsewhere (Lerondel *et al.*, 1996; Setzu *et al.*, 1998).

Illumination setup

Two kind of illumination have been used for photo-induced oxidation of PSi; a focused Gaussian laser beam (120-m-wide spot) and an interferometric pattern produced by overlapping two coherent laser beams. Because of wettability consideration, the PSi sample was immersed in water and ethanol rather than only water during the exposition. In both cases, the $\lambda = 514$ nm line of Argon laser was used as illumination source.

Scanning probe microscopies

SNOM has been used to investigate PL modification after oxidation. The SNOM is based on a tuning fork configuration. Images were obtained in collection mode with a polymer tip grown on a fibre (Bachelot *et al.*, 2001). The tip was metallized and the apex opened using a focus ion beam setup to obtain a 50-nm aperture. SNOM photoluminescence images were obtained through a photomultiplicator associated to a high pass filter to reject the exciting laser wavelength (405 nm), the image obtained is an integral over the whole luminescence spectrum above the exciting wavelength. Moreover, a spectrometer was coupled to the SNOM to get local spectrum of the sample PL. In addition to the tuning fork topographic images, AFM in tapping mode was used with ultra-sharp silicon tip (POINTPROBE® PLUS, by NANOSENSOR, Nanosensor Technology, Boston, MA, USA cantilever length: 225 μm and force constant: 48 N/m, tip radius <7 nm).

Results and discussions

Focused laser beam

A 'type A' sample has been exposed under a focused beam during 15 min. As the illumination profile was Gaussian shaped, this single exposition allows us for the study of the influence of the incident dose on the PL. The spot was expected to be 120 μm wide. Figure 1 shows topographic and PL images of the photo-induced structure. The focusing system induced strong diffraction phenomena leading to the observed annular fringes. The configuration provides a topographic

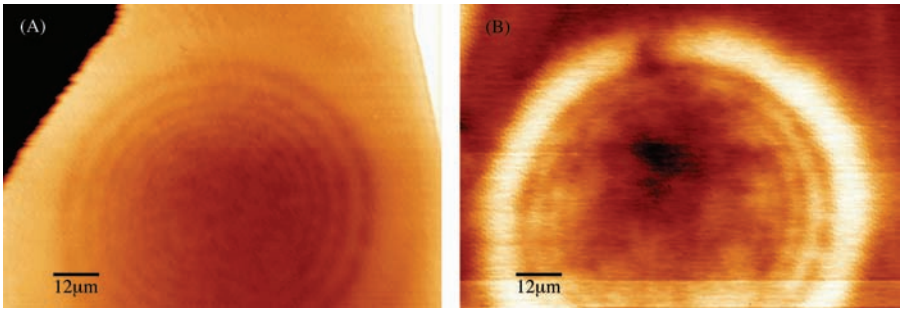

Fig. 1. (A) tuning fork image, (B) SNOM image of a photo-generated structure obtained using a focalized laser beam after 15 min exposure time at 1 mW.

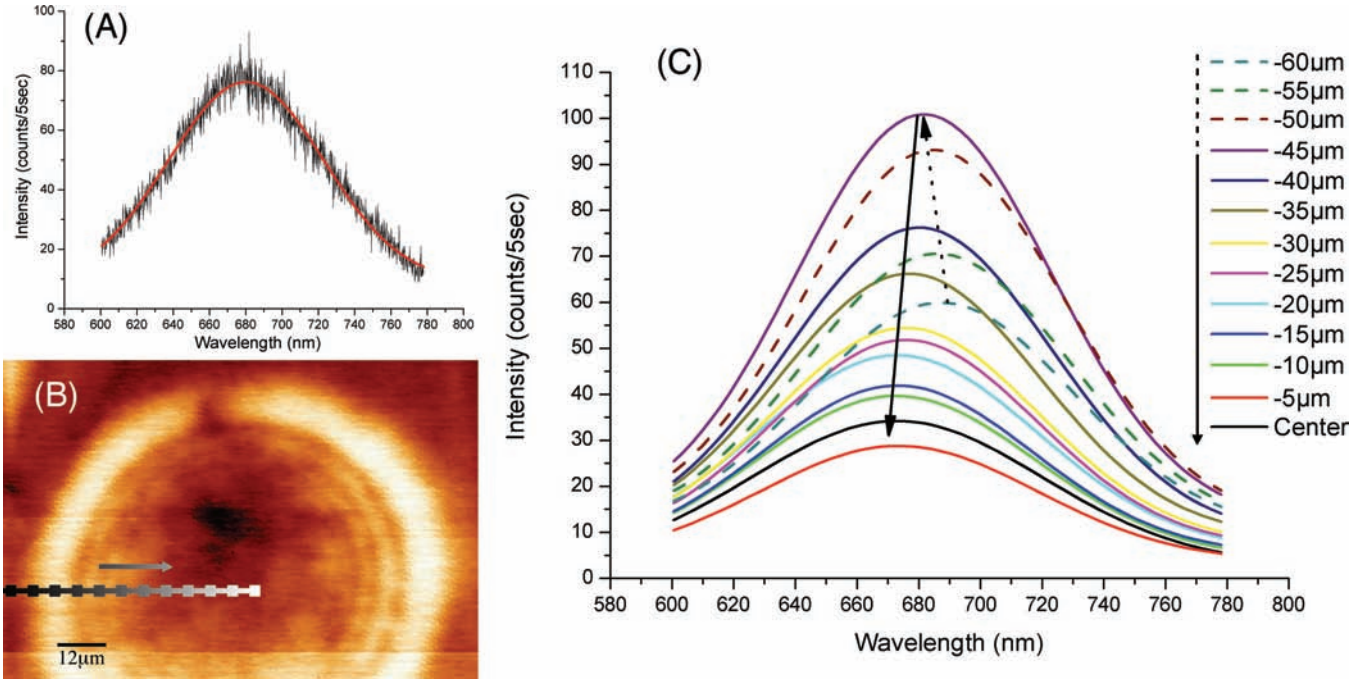

Fig. 2. (A) Raw photoluminescence spectra (black) and Gaussian fit (red), (B) SNOM image, and (C) fitted local photoluminescence spectrum obtained on several points of the pattern [materialized on (B) by the squares]. The arrows in (B) and (C) are guide for the eye to emphasize the evolution of the photoluminescence spectra as we move from the edge to the centre.

image (Fig. 1A), and in the same time a PL image (Fig. 1B). These images show qualitatively the modification induced by the oxidation on both topography and emission properties of the sample. The oxidation has similar effect on both topography and PL of the sample. Moreover, the pattern observed is consistent with the illumination geometry (beam profile of the illumination is not represented here for the sake of clarity).

In addition to these images, a spectrometer has been used to retrieve local PL spectrum on different points (13 points) of the obtained structure (Fig. 2). A raw spectra and its Gaussian fit are presented (Fig. 2A), the other spectrum have been fitted using different parameters, only the fits are presented. The fit error is around 2% for each spectrum. The PL spectra taken on different points along the photo-generated structure show strong modification of emission properties (Fig. 2C). Both the maximum intensity and the wavelength at maximum are modified. Considering that the PSi sample was initially nonphotoluminescent, oxidation is thus believed to modify the PSi layer enough to induce PL.

To get a closer look on the emission properties modification, PL parameters have been plotted as a function of the position on the structure (Fig. 3). As expected with the SNOM image, the PL peak shows a maximum on the edge of the structure (Fig. 3A). At the same time, the peak gets blue shifted from the edge to the centre (Fig 3B). More precisely, this evolution can be decomposed in two phases. On one hand, the peak is blue shifted from 687 to 672 nm. On the other hand, in the central zone (from –20 to 0 μm) the peak wavelength reaches a saturation (at about 672 nm).

Although no structural and morphological observations were performed *in situ*, the PL behaviour is fully consistent with the quantum confinement model (Cullis & Canham, 1991; Cullis *et al.*, 1997; Cooke *et al.*, 2004) together with Wolkin *et al.*'s (1999) observations. Nanoporous PSi structure can be approximated as a collection of silicon nanocrystallites behaving as quantum dots. During the illumination, the silicon nanocrystallites size decreased owing to the oxidation of Si which is replaced by SiO_2 or SiO_x. As a consequence one expects the PL to be strongly modified both in intensity and in wavelength. Let us try now to figure out in more details the process at the origin of these modifications. Recent works (Martín-Palma *et al.*, 2002, 2005) confirm that the nanocrystallite size distribution is well described by a Gaussian. The prepared PSi samples were initially nonphotoluminescent, meaning that the nanocrystallites are not small enough to induce PL. Under illumination, faster oxidation can be locally induced. As previously observed (Cooke *et al.*, 2004) the size modification of the nanocrystallites have drastic effects on the PL. Thus, during the first stage of the oxidation, the size reduction would have been enough to turn few (the smaller ones) nanocrystallites photoluminescent, leading to a low PL signal. As the oxidation occurs, more and more nanocrystallites reach the critical size, the global PL then increases. On the other hand, if the oxidation is too strong the silicon nanocrystallite will be fully oxidized leading to the

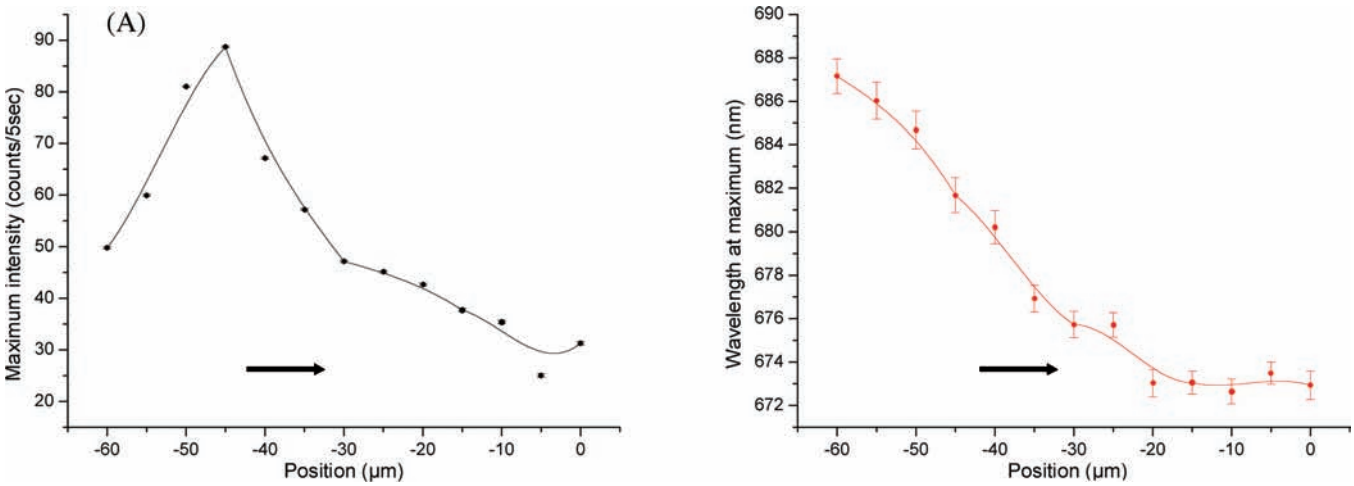

Fig. 3. (A) Maximum intensity and (B) wavelength at the maximum intensity of the photoluminescence versus the position. Curves are guide for the eye, and the arrows used in Fig. 2 are reminders.

extinction of the PL, this phenomenon took place at the centre of the spot where the intensity was maximum. According to the quantum confinement, besides the intensity modification, the size reduction of the nanocrystallite must induce a blue shift of the PL (if there is any). However this blue shift can only be observed to some extend. For oxidized PSi both quantum confinement and surface passivation have to determine the electronic states of the silicon quantum dots. For the smaller crystallites, localized states associated to Si = O bonds have been evoked (Wolkin *et al.*, 1999).

To summarize, during the oxidation process, together with a blue shift, one expect the PL intensity first increases up to a maximum and then decreases. This behaviour is in qualitative agreement with the experimental observations (Figs 2 and 3). Both intensity and blue shift suggest that the oxidation must have been stronger in the central zone, which is consistent with the intensity distribution.

Concerning the oxidation depth, previous works on absorption of PSi (Lerondel *et al.*, 2000) give a typical value of the absorption (0.3–0.4 μm^{-1}) for a 'type A' sample, corresponding to penetration depth of light of 2.5–3.3 μm. As the porous layer thickness (200 nm) is small compared to penetration depth, the material is thus homogenous and the photo-induced oxidation occurs thorough the layer. At the same time it is difficult to analyse the oxidation rate after 15-min exposure time. Based on previous work on passive oxidation (without illumination) of 'type B' samples, we have an approximation of the required time (30 min) to fully oxidize a 200-nm-thick PSi layer. We believed that the oxidation rate is higher than 50% at the centre of the exposed area. Yet, work is in progress to specify the evolution of the oxidation rate with exposure time.

AFM images of the photo-generated structure are presented Fig. 4, they present better resolution compared with shear force images. The topographic modifications of the sample are quite similar to the illumination pattern, as previously observed. The height profile of the photo-generated structure, presented Fig. 4(B), shows height shift between exposed and nonexposed area. The oxidation process relying on the oxidation of Si to SiO_2 the global volume of the nanocrystallite is believed to increase inducing the observed topographic modifications.

Interferometric pattern

The aim was to achieve large-scale photo structuring of PSi in water with better control of illumination geometry, thus we used an interferometric setup. As seen before, the oxidation kinetics can be locally enhanced with illumination, but for the interferometric illumination the incident power density is lower than in the case of the focused beam. Exposure time are then hours long. Pattern stability was thus critical.

After oxidation on 'type B' samples, the sample was imaged by SNOM (Fig. 5A) and AFM (Figs 5B and C). The topography was too smooth to be visible by our shear force microscopy. According to the AFM image the topographic pattern is approximately 10-nm deep, and the period is 7.3 μm. The photo oxidation can be driven with large-scale illumination pattern. Moreover, the oxidation induces topographic modification, in particular the size enhancement of $Si–SiO_x$ cluster with the oxidation. For strong oxidation rate, the pore size can be locally modified consequently to the strong topographic modification and especially the swelling of the $Si–SiO_x$ cluster.

Concerning the resolution, our setup is for the moment not stable enough to lead experiment on the minimal theoretical value of the spatial period of $(\lambda/2n)$ where n is the water refraction index. Indeed, for submicrometreic spatial value, the exposition duration (approximately 2 h) and the stability are not compatible. Nevertheless, a new approach based on a

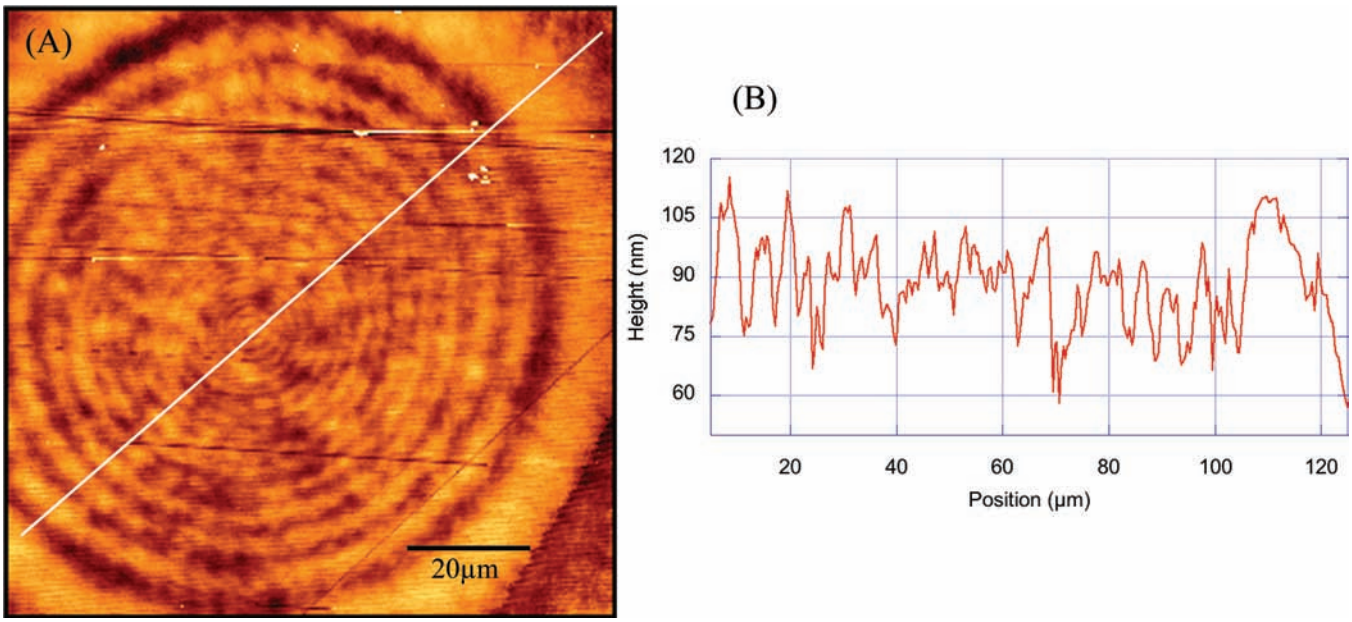

Fig. 4. (A) AFM image, and (B) height profile of the photo generated structure. The profile was retrieved along the white line in (A).

near-field illumination is under consideration to work on the oxidation process at the nanoscale.

Conclusions

In summary, oxidation process induces both topographic and PL modification. This oxidation can be driven by the illumination conditions. Local tuning of the PL is then achievable. Near-field imaging (both topographic and PL imaging) of photo-generated structures shows strong local modification of the topography and the PL spectra. Previous work shows the feasibility of structuring PSi at the nanoscale by photo etching (Diesinger *et al.*, 2002). Photo oxidation of PSi in water offers an alternative method to pattern PSi sample at the nanoscale.

Acknowledgements

M. Juan and J.-S. Bouillard's PhD researches are supported by the European Social Fund and, respectively, the Conseil Général de l'Aube (district grant) ant the région Champagne Ardennes (province grant). The Conseil Régional Champagne-Ardennes is acknowledged for financial support (Projet émergence 'Photostrucutration en champ proche de nouvelles particules hybrides pour la nanophotonique').

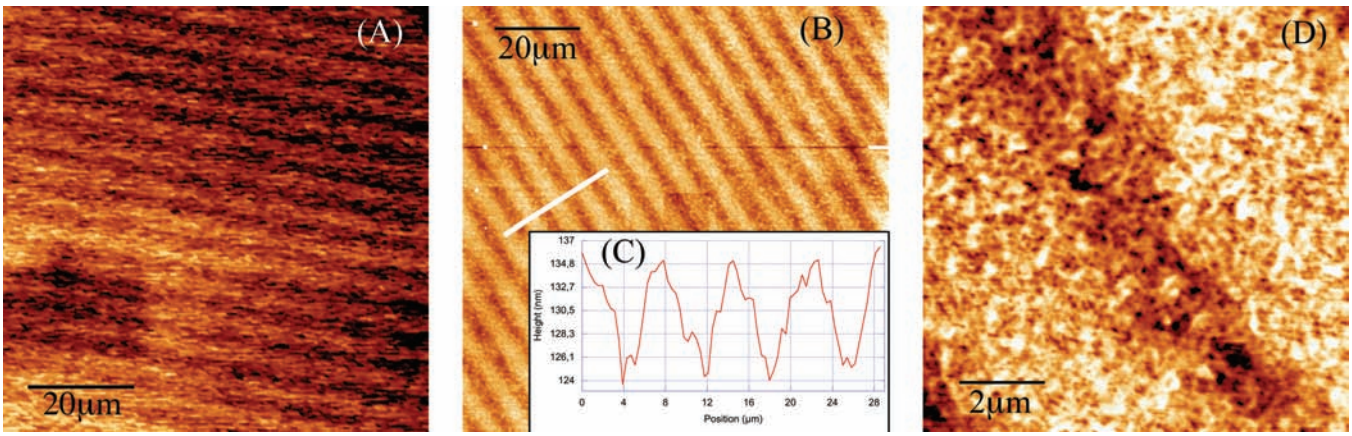

Fig. 5. (A) SNOM image, (B) and (D) AFM images of a photo generated 2D grating obtain by interferometric illumination. (C) is the height profile retrieve from (B) along the white line.

References

Bachelot, R., Ecoffet, C., Deloeil, D., Royer, P. & Lougnot, D.-J. (2001) Integration of micrometer sized polymer elements at the end of optical fibers by free-radical photopolymerization. *Applied Optics* **40**(32), 5760–5871.

Bsiesy, A., Muller, F., Ligeon, M., Gaspard, F., Herino, R., Romestain, R. & Vial, J.C. (1993) Voltage-controlled spectral shift of porous silicon electroluminescence. *Phys. Rev. Lett.* **71**(4), 637–640.

Canham, L.T. (1990) Silicon quantum wire array fabrication by electrochemical and chemical dissolution of wafer. *Appl. Phys. Lett.* **57**(3) 1046–1048.

Cooke, D.W., Muenchausen, R.E., Bennett, B.L., Jacobsohn, L.G. & Nastasi, M. (2004) Quantum confinement contribution to porous silicon photoluminescence spectra. *J. Appl. Phys.* **96**(1), 197–203.

Cullis, A.G. & Canham, L.T. (1991) Visible light emission due to quantum size effects in highly porous crystalline silicon. *Nature* **353**(6342), 38.

Cullis, A.G., Canham, L.T. & Calcott, P.D.J. (1997) The structural and luminescence properties of porous silicon. *J. Appl. Phys.* **82**(3), 309–317.

Diesinger, H., Bsiesy, A. & Hérino, R. (2002) Nano-structuring of silicon and porous silicon by photo-etching near field optics. *Phys. Stat. Sol.* **197**(2), 561–565.

Juan, M., Bouillard, J.S., Plain, J., Bachelot, R., Adam, P.M., Lerondel, G. & Royer, P. (2007) Soft photo structuring of porous silicon in water. *Phys. Stat. Sol. (A)* **204**(5), 1276–1280.

Koropecki, R.R., Arce, R.D. & Schmidt, J.A. (2004) Photo-oxidation effects in porous silicon luminescence. *Phys. Rev. B* **69**(20), 205317-1–205317-6.

Lerondel, G., Ferrand, P. & Romestain, R. (1997) Elaboration and light emission properties of low doped p-type porous silicon microcavities. *Mater. Res. Soc. Symp. Proc.* **452**, 711–716.

Lerondel, G., Thönissen, M., Romestain, R. & Vial, J.C. (1997a) Porous silicon lateral superlattices. *Appl. Phys. Lett.* **71**(2), 196–197.

Lerondel, G., Setzu, S., Thönissen, M. & Romestain, R. (1997b) Holography in porous silicon. *J. Imaging Sci. Technol.* **41**(5), 468–471.

Lerondel, G., Madéore, F., Romestain, R. & Muller, F. (2000) Direct determination of the absorption of porous silicon by photocurrent measurement at low temperature. *Thin Solid Film* **366**, 216–264.

Martín-Palma, R.J., Pascual, L., Herrero, P. & Martínez-Duart, J.M. (2002) Direct determination of grain sizes, lattice parameters, and mismatch of porous silicon. *Appl. Phys. Lett.* **81**(1), 25.

Martín-Palma, R.J., Pascual, L., Herrero, P. & Martínez-Duart, J.M. (2005) Monte Carlo determination of crystallite size of porous silicon from x-ray bad broadening. *Appl. Phys. Lett.* **87**(25), 1–3.

Setzu, S., Lerondel, G. & Romestain, R. (1998) Temperature effect on the roughness of the formation interface p-type porous silicon. *J. Appl. Phys.*, **84**(6), 3129–3133.

Vial, J.C., Briesy, A., Gaspakd, F., Merímo, R., Ligeon, M., Muller, F., Ramestain, R. & Macfarlane, R.M. (1992) Mechanism of visible-light emission from electro-oxidized porous silicon. *Phys. Rev. B.* **45**(24), 14171–14176.

Wolkin, M.V., Jorne, J., Fauchet, P.M., Allan, G. & Delerue, C. (1999) Luminescence in porous silicon quantum dots: the role of oxygne. *Phys. Rev. Lett.* **82**(1), 197–200.

